



**HAL**  
open science

## Energy transport for thick holographic branes

Constantin P. Bachas, Stefano Baiguera, Shira Chapman, Giuseppe Policastro, Tal Schwartzman

► **To cite this version:**

Constantin P. Bachas, Stefano Baiguera, Shira Chapman, Giuseppe Policastro, Tal Schwartzman. Energy transport for thick holographic branes. *Physical Review Letters*, 2023, 131 (2), pp.021601. 10.1103/PhysRevLett.131.021601 . hal-03920869

**HAL Id: hal-03920869**

**<https://hal.science/hal-03920869v1>**

Submitted on 15 Nov 2024

**HAL** is a multi-disciplinary open access archive for the deposit and dissemination of scientific research documents, whether they are published or not. The documents may come from teaching and research institutions in France or abroad, or from public or private research centers.

L'archive ouverte pluridisciplinaire **HAL**, est destinée au dépôt et à la diffusion de documents scientifiques de niveau recherche, publiés ou non, émanant des établissements d'enseignement et de recherche français ou étrangers, des laboratoires publics ou privés.



Distributed under a Creative Commons Attribution 4.0 International License

## Energy Transport for Thick Holographic Branes

Constantin Bachas<sup>1,\*</sup>, Stefano Baiguera<sup>2,†</sup>, Shira Chapman<sup>2,‡</sup>,  
Giuseppe Policastro<sup>1,§</sup> and Tal Schwartzman<sup>2,||</sup>

<sup>1</sup>*Laboratoire de Physique de l'École Normale Supérieure, CNRS, PSL Research University and Sorbonne Universités, 24 rue Lhomond, 75005 Paris, France*

<sup>2</sup>*Department of Physics, Ben-Gurion University of the Negev, David Ben Gurion Boulevard 1, Beer Sheva 84105, Israel*

 (Received 3 February 2023; revised 20 April 2023; accepted 22 June 2023; published 11 July 2023)

Universal properties of two-dimensional conformal interfaces are encoded by the flux of energy transmitted and reflected during a scattering process. We develop an innovative method that allows us to use results for the energy transmission in thin-brane holographic models to find the energy transmission for general smooth domain-wall solutions of three-dimensional gravity. Our method is based on treating the continuous geometry as a discrete set of branes. As an application, we compute the transmission coefficient of a Janus interface in terms of its deformation parameter.

DOI: [10.1103/PhysRevLett.131.021601](https://doi.org/10.1103/PhysRevLett.131.021601)

*Introduction and summary.*—Defects and interfaces are important probes in quantum field theory and also ubiquitous in condensed-matter physics. They include such diverse systems as junctions of quantum wires, constrictions of quantum Hall liquids, or impurities in quantum spin chains and ultracold atomic gases; see, e.g., [1–11]. Many of these systems exhibit physical phenomena that are not present when the theory is weakly coupled, and it is important to develop analytic tools to study them. In this Letter, we use the AdS/CFT correspondence [12], which provides a dictionary between strongly coupled field theories and gravitational systems, to calculate the transmission of energy through a large class of interfaces with holographic duals.

We focus on conformal interfaces between two 2D conformal field theories,  $CFT_L$  and  $CFT_R$ . Folding along the interface gives a theory living on half-space with two energy-momentum tensors,  $T_L$  and  $T_R$ , which are separately conserved in the bulk. Their sum  $T_{\text{tot}} = T_L + T_R$  is also conserved at the interface, but this is not true in general for the other spin-2 current,  $T_{\text{rel}} = c_R T_L - c_L T_R$ , where  $c_L$ ,  $c_R$  are the central charges of the two CFTs. As shown in Ref. [13], the fraction of energy transported across such 2D interfaces is universal, i.e., the same for all incident excitations, and controlled by a parameter  $c_{LR}$  that appears in the two-point function of  $T_{\text{rel}}$  [14,15]. Explicitly,

$$c_{LR} = c_L \mathcal{T}_L = c_R \mathcal{T}_R, \quad (1)$$

with  $\mathcal{T}_L(\mathcal{T}_R)$  the fraction of transmitted energy for excitations hitting the interface from the left (right). Note that the second equality in (1) is the condition for detailed balance. Together with the ground-state entropy  $\log g$  [16],  $c_{LR}$  is an important parameter of any 2D interface CFT (ICFT).

Holographic studies of energy transport [17,18] were so far limited to toy models involving thin branes anchored on the boundary of anti-de Sitter (AdS) spacetime [19–22]. In this Letter, we will move from these *ad hoc* models to a whole new arena of holographic interfaces described by smooth (super)gravity solutions, which we refer to as thick branes; see, e.g., [23–29]. Such solutions have well-defined, rather than hypothetical, dual ICFTs, thus placing the analysis on much firmer ground.

While the entanglement entropy, complexity, and other quantum-information measures were extensively studied in holography for both thin-brane models and for smooth solutions [30–46], less attention has been paid to energy transport and to the parameter  $c_{LR}$ . For a single thin brane separating two patches of  $\text{AdS}_3$ , this parameter was first computed in Ref. [17] with the result

$$c_{LR} = \frac{3}{G} \left( \frac{1}{\ell_L} + \frac{1}{\ell_R} + 8\pi G\sigma \right)^{-1}, \quad (2)$$

where  $\sigma$  is the brane tension,  $G$  is the three-dimensional Newton constant, and  $\ell_L, \ell_R$  are the asymptotic  $\text{AdS}_3$  radii, related to the central charges by the Brown-Henneaux formula [47]  $c = 3\ell/2G$ . The above result was confirmed in Ref. [48] from nonequilibrium steady states of the thin-brane model. Our goal here is to compute  $c_{LR}$  for general two-dimensional ICFTs that admit a smooth holographic dual of three-dimensional gravity coupled to any kind of matter.

Published by the American Physical Society under the terms of the [Creative Commons Attribution 4.0 International license](https://creativecommons.org/licenses/by/4.0/). Further distribution of this work must maintain attribution to the author(s) and the published article's title, journal citation, and DOI. Funded by SCOAP<sup>3</sup>.

We bypass the computationally involved nature of the problem by treating the geometry as a discrete set of thin branes. Our argument is inspired by the observation [18] (see also [48]) that transmission past a pair of interfaces modeled by thin branes with tensions  $\sigma_1, \sigma_2$  is the same as for a single thin brane with tension  $\sigma_1 + \sigma_2$ . That is, the transmission is additive in the tensions.

The  $SO(2,1)$  symmetry of the ICFT ground state implies that the dual geometry is a warped product  $\mathbb{R} \times_w \text{AdS}_2$ , and that all matter-field backgrounds only depend on the proper-distance coordinate  $y$  on  $\mathbb{R}$ . It follows that the matter energy-momentum tensor can be written as

$$T_{\mu\nu}^{\text{matter}} = -\Lambda g_{\mu\nu} - \frac{d\sigma}{dy} \Pi_{\mu\nu}, \quad (3)$$

where  $\Pi_{\mu\nu}$  is a projector on  $\text{AdS}_2$  and  $\Lambda$  and  $d\sigma/dy$  are functions only of  $y$ . They are the vacuum energy and tension density of our brane array. We must assume that  $\Lambda(y)$  is everywhere negative, so that between two branes the geometry is always AdS. We argue that for such solutions  $c_{LR}$  is still given by Eq. (2) with the replacements

$$\sigma \rightarrow \int_{-\infty}^{\infty} \frac{d\sigma}{dy} dy \quad \text{and} \quad \begin{cases} \ell_L \rightarrow 1/\sqrt{-\Lambda(-\infty)}, \\ \ell_R \rightarrow 1/\sqrt{-\Lambda(\infty)}. \end{cases} \quad (4)$$

This follows from iterating the additivity argument of [18] and approximating (3) by a dense array of thin branes with tensions  $d\sigma$ . The above simple formula for  $c_{LR}$  in terms of the dual geometry is the main result of the Letter.

We verified, using as matter a scalar field, that the above result obeys the bounds following from the average-null-energy condition (ANEC) [13]

$$0 \leq c_{LR} \leq \min(c_L, c_R), \quad (5)$$

i.e., the condition that both the reflected and the transmitted energies are always positive. We further show that, in contrast to the thin-brane model, these bounds can be saturated. Total reflection, in particular, is possible without depleting the degrees of freedom of one side, as in Ref. [17].

A key part of the argument leading to the result (2)–(4) is that  $c_{LR}$  can be extracted from transverse-traceless graviton modes in  $\text{AdS}_2$ , whose linearized wave equation depends only on the geometry, not on the matter-field backgrounds [49,50]. Since the thin-brane discretization reproduces (by construction, as we will see) the smooth background geometry in the continuum limit, it should also give the same linear scattering of transverse-traceless modes.

The results of this Letter could be of use to a large fraction of the physics community, both condensed-matter theorists modeling strongly coupled interfaces and defects and those interested in quantum gravity and holography. The relation between entanglement and energy transfer is, for example, important in recent calculations of quantum

extremal surfaces and islands, where both thin-brane toy models and thick branes have been employed [51–58]. On a different note, a double Wick rotation converts our thin-brane array to a cosmology of discrete quenches at which the Hubble parameter jumps. It could be interesting to explore if such a discretization can help calculate the cosmological production and evolution of gravity waves.

*AdS domain walls.*—Consider Einstein gravity coupled to a scalar field—the extension to arbitrary matter will be straightforward. The action, in units  $8\pi G = 1$ , reads

$$I_{\text{gr}} = \frac{1}{2} \int d^{n+1}x \sqrt{-g} [R - \partial^\mu \phi \partial_\mu \phi - 2V(\phi)]. \quad (6)$$

The dimension  $n+1$  is arbitrary for now. We later set  $n=2$ . Solutions dual to vacuum ICFTs depend on a space coordinate  $y \equiv x^n$  such that (with  $\alpha, \beta = 0, \dots, n-1$ )

$$\phi = \phi(y), \quad ds^2 = dy^2 + a^2(y) \bar{\gamma}_{\alpha\beta} dx^\alpha dx^\beta, \quad (7)$$

and  $\bar{\gamma}_{\alpha\beta}$  is the metric of unit-radius  $\text{AdS}_n$ . It is convenient to define the conformal coordinate  $\theta$ , such that  $ad\theta = dy$  and

$$ds^2 = a^2(\theta) (d\theta^2 + \bar{\gamma}_{\alpha\beta} dx^\alpha dx^\beta). \quad (8)$$

The field  $\phi(y)$  and scale factor  $a(y)$  obey

$$\frac{n(n-1)}{2} \left[ \left( \frac{a'}{a} \right)^2 - \frac{k}{a^2} \right] = \frac{1}{2} (\phi')^2 - V(\phi) \quad (9)$$

$$\text{and} \quad \phi'' + n\phi' \frac{a'}{a} - \frac{dV}{d\phi} = 0, \quad (10)$$

where  $k = -1$  is the curvature of  $\bar{\gamma}_{\alpha\beta}$ , primes denote derivatives with respect to  $y$ , and  $V(\phi)$  is the potential. At a critical point  $\phi_c$  of  $V$ , the solution

$$\phi = \phi_c \quad \text{and} \quad a = \frac{\ell}{\cos \theta} = \ell \cosh(y/\ell) \quad (11)$$

describes pure  $\text{AdS}_{n+1}$  spacetime of radius  $\ell$ , where  $V(\phi_c) = -n(n-1)/2\ell^2$ . Domain-wall solutions interpolate between critical points.

A double Wick rotation,  $y \rightarrow it$  and  $\text{AdS}_n \rightarrow \text{EAdS}_n$  converts Eqs. (9) and (10) to the familiar equations for an open, homogeneous, and isotropic universe coupled to an inflaton  $\phi$  [59]. Another related context [60–62], with  $k=0$ , describes holographic renormalization-group flows triggered by an operator dual to  $\phi$ .

Here we are interested in AdS domain walls with metric given by (8). Figure 1 shows a typical geometry parametrized by  $(z, \theta)$  with  $z \equiv x^1$  the radial Poincaré coordinate of  $\text{AdS}_n$  (i.e.,  $\bar{\gamma}_{\alpha\beta} = \eta_{\alpha\beta}/z^2$ ). For pure  $\text{AdS}_{n+1}$ ,  $(z, \theta)$  are polar coordinates on the  $(\xi, u)$  plane, with  $\xi$  the radial Poincaré coordinate of  $\text{AdS}_{n+1}$  and  $u$  the coordinate transverse to the would-be interface. More generally,  $\theta$

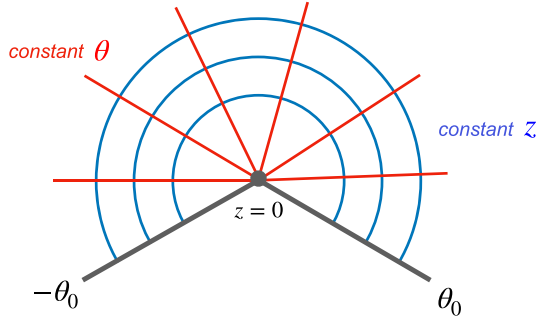


FIG. 1. Foliation of the Janus geometry by  $\text{AdS}_n$  fibers with radial Poincaré coordinate  $z$ . The dual CFT interface is located at  $z = 0$ , whereas the conformal boundary also includes  $\theta = \pm\theta_0$ , where  $a(\theta)$  diverges.

takes values in an interval  $(-\theta_0, \theta_0)$ , the field  $\phi(\theta)$  approaches critical points  $\phi_L$  and  $\phi_R$  of  $V$  at the two extremes, and

$$a(-\theta_0 + \delta\theta) \simeq \frac{\ell_L}{\delta\theta}, \quad a(\theta_0 - \delta\theta) \simeq \frac{\ell_R}{\delta\theta}, \quad (12)$$

with  $\ell_L, \ell_R$  the asymptotic  $\text{AdS}_{n+1}$  radii.

A simple example of holographic ICFT for  $n = 2$  is the Janus solution found in [24,25]. In this case, the asymptotic radii are  $\ell_L = \ell_R \equiv L$  and  $\phi$  is the dilaton that is dual to a marginal operator, so that  $V(\phi) \equiv -1/L^2$  is constant. Equation (10) then shows that  $\phi'a^2$  is also constant. Inserting in Eq. (9) gives

$$a = \frac{L}{\sqrt{2}} [1 + (1-b) \cosh(2y/L)]^{1/2}, \quad (13a)$$

$$\phi = \phi_0 + \frac{1}{\sqrt{2}} \log \left[ \frac{\sqrt{2-b} + \sqrt{b} \tanh(y/L)}{\sqrt{2-b} - \sqrt{b} \tanh(y/L)} \right], \quad (13b)$$

where  $0 \leq b \leq 1$  ( $b \equiv 1 - \sqrt{1 - 2\gamma^2}$  comparing with the conventions of [25]). As before, we can trade  $y$  for  $\theta$ , satisfying  $d\theta = dy/a$ . As  $y$  ranges from  $-\infty$  to  $\infty$ ,  $\theta$  varies from  $-\theta_0$  to  $\theta_0$ , where

$$\theta_0 = \left(1 - \frac{b}{2}\right)^{-1/2} K\left(\frac{b}{2-b}\right) \geq \pi/2, \quad (14)$$

with  $K$  the complete elliptic integral of the first kind. For  $b = 0$ , the dilaton is constant and the geometry is pure  $\text{AdS}_3$ , whereas for  $b = 1$ , the dilaton is linear and the geometry is  $\mathbb{R} \times \text{AdS}_2$ . More generally, the arbitrary parameters  $\phi_0$  and  $b$  can be traded for  $\phi(\pm\theta_0)$ , the marginal couplings of the CFT on the two sides of the interface.

The Janus solution (13a) and (13b) can be embedded in type IIB supergravity compactified on  $\text{AdS}_3 \times S^3 \times T^4$  or  $\text{AdS}_3 \times S^3 \times K3$ , but it is nonsupersymmetric and possibly unstable. In addition to activating more fields,

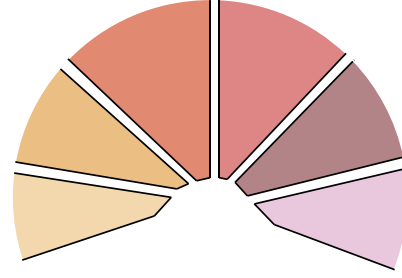


FIG. 2.  $N_\epsilon$  regions of  $\text{AdS}_{n+1}$  spacetime glued together along thin branes. In the continuum limit  $\epsilon \rightarrow 0$ , this geometry will match the smooth solution.

supersymmetric solutions have a nontrivial dependence on the extra dimensions [27–29]. Our discussion below will *a priori* apply only after this dependence has been smeared, or better if the reduction to  $n + 1$  dimensions is a consistent truncation.

*Matter as a thin-brane array.*—Now the key idea is to replace the smooth solutions by a “pizza” of  $\text{AdS}_n$  slices separated by thin tensile branes; see Fig. 2. We divide the range of  $\theta$  into  $2N_\epsilon$  intervals of size  $\epsilon$  (so that  $\epsilon N_\epsilon = \theta_0$ ), and let the metric in the  $j$ th interval be  $\text{AdS}_{n+1}$  with radius  $\ell_j$ . The label  $j$  runs from  $-N_\epsilon + 1$  to  $N_\epsilon$ . In the  $j$ th interval, the modified scale factor  $\tilde{a}$  reads

$$\tilde{a}(\theta) = \frac{\ell_j}{\cos(\theta - \delta_j)} \quad \text{for } (j-1)\epsilon < \theta < j\epsilon. \quad (15)$$

Furthermore, the two end point values of each interval are fixed to be those of the original solution,  $\tilde{a}(j\epsilon) = a(j\epsilon) \equiv a_j$  for all  $j$ .

Using Eq. (15), we can express  $\ell_j$  and the shift  $\delta_j$  in terms of the radii of the  $\text{AdS}_n$  branes  $a_j$  and  $a_{j-1}$ . The  $\ell_j$  will *a priori* jump from one interval to the next, and we attribute this jump to thin-brane sources with tension  $\sigma_j$ , localized at  $\theta = j\epsilon$ . The Israel junction conditions [63] read (see, e.g., [64])

$$\sigma_j a_j = \sqrt{\left(\frac{a_j}{\ell_j}\right)^2 - 1} - \sqrt{\left(\frac{a_j}{\ell_{j+1}}\right)^2 - 1}, \quad (16)$$

for  $\ell_{j+1} > \ell_j$  (otherwise the sign of the rhs should be flipped to maintain positive tension). Equation (16) expresses  $\sigma_j$  in terms of  $a_j$ ,  $\ell_j$ , and  $\ell_{j+1}$  or, using (15), in terms of the three scale factors  $a_{j-1}$ ,  $a_j$ , and  $a_{j+1}$ .

By construction, the discretized (tilde) geometry approaches the smooth ICFT solution as  $\epsilon \rightarrow 0$ . Both  $\ell_j$  and  $\delta_j$  approach smooth functions  $\ell(\theta)$  and  $\delta(\theta)$  in the limit, while  $\sigma_j/\epsilon$  tends (as a distribution) to a tension density  $d\sigma/d\theta$ . From Eqs. (15) and (16),

$$\ell = \frac{a}{\sqrt{1 + (\dot{a}/a)^2}}, \quad \tan(\theta - \delta) = \frac{\dot{a}}{a} \quad (17a)$$

$$\text{and } \frac{d\sigma}{d\theta} = \frac{a|\dot{\ell}'|}{\ell^2\sqrt{a^2 - \ell^2}}, \quad (17b)$$

where dots stand for derivatives with respect to  $\theta$ .

Since the discretized geometry obeys the Einstein equations, its source should also converge to the energy-momentum tensor of the smooth solution. For a single scalar field, we have

$$T_{\mu\nu}^\phi = -(\partial^\rho\phi\partial_\rho\phi)\Pi_{\mu\nu} + g_{\mu\nu}\left(\frac{1}{2}\partial^\rho\phi\partial_\rho\phi - V\right), \quad (18)$$

where  $\Pi_{\mu\nu} = g_{\mu\nu} - \hat{n}_\mu\hat{n}_\nu$  projects onto hypersurfaces of constant  $\phi$  (with  $\hat{n}_\mu$  the unit normal vector field). Comparing to the thin-brane array, which includes a piecewise-constant vacuum energy  $\Lambda = -1/\ell^2$ , we get

$$\Lambda = -\frac{1}{2}(\phi')^2 + V \quad \text{and} \quad d\sigma = (\phi')^2 dy. \quad (19)$$

For the second equality, we used the fact that the energy-momentum tensor of a thin brane of tension  $\lambda$  localized at  $y = y_0$  is  $T_{\mu\nu} = -\lambda\Pi_{\mu\nu}\delta(y - y_0)$  (see, e.g., [65]). Using Eqs. (9) and (10), one can check that the expressions (17) and (19) for  $\Lambda$  and  $d\sigma$  indeed coincide. For the Janus solution (13), we find

$$d\sigma^{\text{Jan}} = \frac{2b(2-b)dy}{L^2[1 + (1-b)\cosh(2y/L)]^2}. \quad (20)$$

Integrating gives the total tension of the brane array

$$\sigma_{\text{tot}}^{\text{Jan}} = \frac{4}{L\sqrt{b(2-b)}} \operatorname{arctanh}\left(\sqrt{\frac{b}{2-b}}\right) - \frac{2}{L}. \quad (21)$$

This vanishes for  $b = 0$ , as it should, and diverges in the opposite limit  $b \rightarrow 1$ .

In approximating the energy-momentum tensor by a thin-brane array, we only relied on the  $\text{AdS}_n$  isometries guaranteeing that  $T_{\mu\nu}^{\text{matter}}$  is a linear combination of  $g_{\mu\nu}$  and  $\hat{n}_\mu\hat{n}_\nu$ , see Eq. (3). Simple algebra leads then to a formula valid in any dimension with any matter content,

$$d\sigma = \left(T_{yy}^{\text{matter}} - \frac{1}{n}\Pi^{\mu\nu}T_{\mu\nu}^{\text{matter}}\right)dy. \quad (22)$$

We now focus on  $n = 2$  and explain why the above tension density controls the energy transport.

*Scattering off a thin-brane array.*—The discretized geometry makes it possible to exploit the results of Refs. [17,18,48] on energy transport in thin-brane models. For an isolated brane, the classical linearized scattering calculation gives [17]

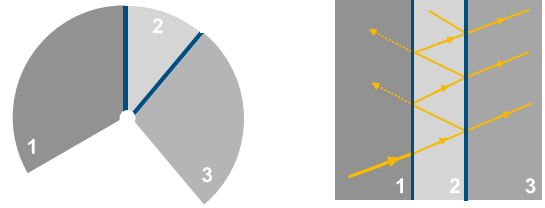


FIG. 3. Fixed-time slice of the brane-pair geometry (left) and the dual boundary ICFT with time running upward (right). The total transmitted energy is the sum over the number  $m$  of double reflections in region 2. The interfaces were infinitesimally separated.

$$\mathcal{T}_{1\rightarrow 2} = \frac{2}{\ell_1} \left( \frac{1}{\ell_1} + \frac{1}{\ell_2} + 8\pi G\sigma \right)^{-1}, \quad (23)$$

where  $\mathcal{T}_{1\rightarrow 2}$  is the fraction of energy incident from side 1 and transmitted to side 2 of the ICFT,  $\ell_{1,2}$  are the AdS radii,  $\sigma$  is the brane tension, and we have restored the  $8\pi G$ . Multiplying by  $c_1$  recovers Eq. (2).

This calculation was extended in Ref. [18] to a pair of thin branes with tensions  $\sigma_{1,2}$ , separating three AdS regions with radii  $\ell_{1,2,3}$ , see Fig. 3. The result is that the tensions add up,

$$\mathcal{T}_{1\rightarrow 3} = \frac{2}{\ell_1} \left( \frac{1}{\ell_1} + \frac{1}{\ell_3} + 8\pi G(\sigma_1 + \sigma_2) \right)^{-1}. \quad (24)$$

Both Eqs. (23) and (24) can be also derived from non-equilibrium steady states if thermostats are attached on either side of the interface [48]. The transport coefficients are in this case extracted by matching the ICFT formula [66,67]

$$c_{LR} = \frac{12J_E}{\pi(\Theta_L^2 - \Theta_R^2)}, \quad (25)$$

where  $J_E$  is the steady flow of heat, and  $\Theta_L$  and  $\Theta_R$  are the temperatures on the left and right of the interface. This calculation in gravity confirms that energy transport in 2D ICFTs is universal [13].

In the ICFT, Eq. (24) can be interpreted as summing over multiple reflections in the middle region, see Fig. 3. Indeed, using (23) one can verify that

$$\begin{aligned} \mathcal{T}_{1\rightarrow 3} &= \mathcal{T}_{1\rightarrow 2}\mathcal{T}_{2\rightarrow 3}[1 + \mathcal{R}_{2\rightarrow 3}\mathcal{R}_{2\rightarrow 1} + \dots \\ &\quad + (\mathcal{R}_{2\rightarrow 3}\mathcal{R}_{2\rightarrow 1})^m + \dots], \end{aligned} \quad (26)$$

where  $\mathcal{R}_{1\rightarrow 2} = 1 - \mathcal{T}_{1\rightarrow 2}$  and  $\mathcal{R}_{2\rightarrow 1} = 1 - \mathcal{T}_{2\rightarrow 1}$ . This calculation is classical, not only in gravity, but also in ICFT. Quantum interference can invalidate the result and lead to singular interface fusion [68], which signals an instability when the anchor points of the branes get close [64]. In the present context we do not expect such instabilities to arise if the original (super)gravity solution was stable before the discretization.

Equation (24) is easy to extend by iteration to any number of adjacent branes. Applying it to the  $\epsilon \rightarrow 0$  limit of the thin-brane array leads to the main result of this Letter, as summarized by Eqs. (2)–(4) in the Introduction. For the Janus example in the second section, using the total tension Eq. (21) and  $\ell_L = \ell_R = L$  we find

$$\mathcal{T}^{\text{Jan}} = \frac{1}{2} \sqrt{b(2-b)} \left[ \operatorname{arctanh} \left( \sqrt{\frac{b}{2-b}} \right) \right]^{-1}. \quad (27)$$

Note that, as  $b$  varies from 1 to 0,  $\mathcal{T}^{\text{Jan}}(b)$  takes all values in the interval  $[0, 1]$ .

*Bounds.*—As explained in Ref. [17], in the case of a single thin brane the existence of the static vacuum solution requires that the tension lies inside the stability window

$$\left| \frac{1}{\ell_L} - \frac{1}{\ell_R} \right| \leq 8\pi G\sigma \leq \frac{1}{\ell_L} + \frac{1}{\ell_R}. \quad (28)$$

Inserting these inequalities in Eq. (2) shows that the ANEC bounds (5) are automatically obeyed. As stressed, however, in Ref. [18], the upper bound in (28) implies (for finite central charges) a positive lower bound on  $c_{LR}$ , so that the thin-brane model does not cover the entire range allowed by ANEC.

For the thin-brane array studied here, the stability window in the continuum limit becomes

$$\left| \frac{d}{dy} \frac{1}{\ell(y)} \right| \leq 8\pi G \frac{d\sigma}{dy} \leq \infty. \quad (29)$$

The upper bound is trivial because the tension  $d\sigma$  is infinitesimal, whereas the local AdS radius is assumed finite. The lower bound is also automatic for any scalar potential, as can be shown using Eqs. (19), the relation  $\Lambda(y) = -1/\ell(y)^2$ , and the equations of motion (9) and (10). Thus, the ANEC bounds are also automatic. By relaxing, however, the upper limit of the stability window, one can now cover the entire ANEC range. Note that for Janus  $c_L = c_R$ , and the ANEC bound reduces to  $0 \leq \mathcal{T}_L = \mathcal{T}_R \leq 1$ .

*Perturbations.*—It should be, in principle, possible to compute  $c_{LR}$  directly for the thick-brane solution. Without performing the calculation, we will argue that the result is obtained by the  $\epsilon \rightarrow 0$  limit of the thin-brane array.

The scattering states of Ref. [17] are characterized by the expectation values of energy fluxes incident on or coming out of the interface,  $\langle T_L^{\text{in}} \rangle$ ,  $\langle T_R^{\text{in}} \rangle$ ,  $\langle T_L^{\text{out}} \rangle$ , and  $\langle T_R^{\text{out}} \rangle$ . The crucial point is that these can be prepared with metric perturbations that are transverse and traceless in AdS<sub>2</sub>, so that their linearized Einstein equations depend only on the geometry, not on the matter-field backgrounds [49,50]. Leaving for the moment the dimension  $n+1$  arbitrary, consider the perturbation

$$ds^2 = dy^2 + a^2(y) [\bar{\gamma}_{\alpha\beta} + h_{\alpha\beta}] dx^\alpha dx^\beta \\ \text{with } \bar{\gamma}^{\alpha\beta} h_{\alpha\beta} = \bar{\nabla}^\alpha h_{\alpha\beta} = 0. \quad (30)$$

Expanding in AdS <sub>$n$</sub>  harmonics,

$$h_{\alpha\beta}(\mathbf{x}, y) = \sum_r h_{\alpha\beta}(\mathbf{x}|r) \psi_r(y), \quad (31)$$

where  $r$  labels spin-2 representations of SO(2,  $n-1$ ), reduces Einstein's equations to

$$-(a^n \psi_r')' = m_r^2 a^{n-2} \psi_r, \quad (32)$$

where  $m_r$  is the mass of the excitation in the  $r$ th harmonic. For  $n > 2$ , this (Kaluza-Klein) decomposition gives an infinite tower of spin-2 excitations in AdS <sub>$n$</sub>  labeled by  $n-1$  momenta and by the mass, or equivalently, the scaling dimension in the dual CFT,  $m_\Delta^2 = \Delta(\Delta - n + 1)$ . In the absence of the interface, the spectrum is  $\Delta = n, n+1, \dots$ . This is the decomposition of the massless spin-2 representation of SO(2,  $n$ ) under SO(2,  $n-1$ ) [19,50]. Note that the massless AdS <sub>$n+1$</sub>  particle gives a tower of massive AdS <sub>$n$</sub>  states.

The case  $n = 2$  is special because the three-dimensional graviton only has surface excitations. As a result, for a given frequency  $\omega$  the tower collapses to a pair of modes, both of them massless in AdS<sub>2</sub> ( $\Delta = 1$ ) [69]. They can be written explicitly as follows:

$$h_{\pm\pm}(\mathbf{x}, y) = e^{i\omega(x^0 \pm x^1)} \left[ A_\pm^\omega + B_\pm^\omega \int^y \frac{d\tilde{y}}{a(\tilde{y})^2} \right], \quad (33)$$

where  $A_\pm^\omega B_\pm^\omega$  are constants of integration of Eq. (32), which is readily solved when  $m_r = 0$ .

We can use the constants  $A_\pm^\omega, B_\pm^\omega$  to fix the two ingoing and two outgoing fluxes in the scattering state. To this end, one must transform to Fefferman-Graham (FG) coordinates, which are not defined globally, but must be chosen separately on the half boundaries  $y = \pm\infty$  (see [32,36,71,72]). Even at leading order in  $h_{\alpha\beta}$  these reparametrizations are cumbersome, but the main point, following [17], is that the two FG patches should match across a static interface on the AdS<sub>3</sub> boundary. This ensures the conservation of CFT energy,  $\langle T_L^{\text{in}} \rangle + \langle T_R^{\text{in}} \rangle = \langle T_L^{\text{out}} \rangle + \langle T_R^{\text{out}} \rangle$ , and eliminates one of the four integration constants.

The final equation is a boundary condition at the Poincaré horizon. To obtain it, following again [17], consider the conjugate “momenta”  $\pi_{\alpha\beta} = \sqrt{-\tilde{g}}(K_{\alpha\beta} - \tilde{g}_{\alpha\beta}K)$ , with  $\tilde{g}_{\alpha\beta}$  the metric on fixed- $y$  slices and  $K_{\alpha\beta}$  the extrinsic curvature. We can separate  $\pi_{\alpha\beta}$  in a traceless part  $\hat{\pi}_{\alpha\beta}$  and the trace. At leading order in the perturbation, the “momentum constraint” actually shows that  $\hat{\pi}_{\alpha\beta}$  is also transverse. Thus,  $\hat{\pi}_{\alpha\beta}$  decomposes into two waves, one going in and one coming out of the Poincaré horizon. Setting the outgoing wave to zero,  $\hat{\pi}_{++} = 0$ , gives after a little algebra  $B_+^\omega = 0$ . This condition, once imposed at one value of  $y$ , remains valid for all  $y$ .

The two remaining free parameters are used to fix the incoming energy fluxes in the CFT. The outgoing fluxes

give then the transport coefficients that we set out to compute. The main point about this calculation is that it only involves the scale factor  $a(y)$ , so discretizing it should not change the answer in the continuum limit. Indeed, a convenient way of performing the calculation is by following exactly the steps of [17,18] for the thin-brane array defined in the third section.

*Outlook.*—Several questions left open by our work deserve further study. It would be interesting, in particular, to extend the calculation of  $c_{LR}$  to top-down holographic interfaces that cannot be reduced to Einstein’s equations in three dimensions. Another interesting direction is to find a holographic proof of the fact that the energy-transmission coefficients do not depend on details of the scattering state [13] or to understand if our method can be extended to study the holographic transport of electric charge. Finally, the double Wick rotation mentioned in the second section converts the brane array into a sequence of cosmological quenches between periods of de Sitter expansion. It would be very interesting to understand how our results translate in this context.

We would like to thank Sara Bonansea, Marc Henneaux, Zohar Komargodski, Yaron Oz, and Vassilis Papadopoulos for useful discussions. The work of S. B., S. C., and T. S. is supported by the Israel Science Foundation (Grant No. 1417/21) and by the German Research Foundation through a German-Israeli Project Cooperation (DIP) grant “Holography and the Swampland.” S. B. is grateful to the Azrieli foundation for an Azrieli fellowship. S. C. acknowledges the support of Carole and Marcus Weinstein through the BGU Presidential Faculty Recruitment Fund.

---

\*costas.bachas@ens.fr

†baiguera@post.bgu.ac.il

‡schapman@bgu.ac.il

§giuseppe.policastro@ens.fr

||taljios@gmail.com

- [1] C. L. Kane and M. P. A. Fisher, Transport in a One-Channel Luttinger Liquid, *Phys. Rev. Lett.* **68**, 1220 (1992).
- [2] S. Eggert and I. Affleck, Magnetic impurities in half-integer-spin Heisenberg antiferromagnetic chains, *Phys. Rev. B* **46**, 10866 (1992).
- [3] E. Wong and I. Affleck, Tunneling in quantum wires: A boundary conformal field theory approach, *Nucl. Phys.* **B417**, 403 (1994).
- [4] P. Fendley, A. W. W. Ludwig, and H. Saleur, Exact Conductance through Point Contacts in the  $\nu = 1/3$  Fractional Quantum Hall Effect, *Phys. Rev. Lett.* **74**, 3005 (1995).
- [5] M. Oshikawa and I. Affleck, Boundary conformal field theory approach to the critical two-dimensional Ising model with a defect line, *Nucl. Phys.* **B495**, 533 (1997).
- [6] C. Nayak, M. P. A. Fisher, A. W. W. Ludwig, and H. H. Lin, Resonant multilead point-contact tunneling, *Phys. Rev. B* **59**, 15694 (1999).

- [7] V. I. Fal’ko and S. V. Iordanskii, Topological Defects and Goldstone Excitations in Domain Walls between Ferromagnetic Quantum Hall Liquids, *Phys. Rev. Lett.* **82**, 402 (1999).
- [8] S. Rommer and S. Eggert, Spin- and charge-density oscillations in spin chains and quantum wires, *Phys. Rev. B* **62**, 4370 (2000).
- [9] J. Catani, G. Lamporesi, D. Naik, M. Gring, M. Inguscio, F. Minardi, A. Kantian, and T. Giamarchi, Quantum dynamics of impurities in a one-dimensional Bose gas, *Phys. Rev. A* **85**, 023623 (2012).
- [10] A. Gromov, Geometric defects in quantum Hall states, *Phys. Rev. B* **94**, 085116 (2016).
- [11] Y. Ashida, T. Shi, M. C. Bañuls, J. I. Cirac, and E. Demler, Solving Quantum Impurity Problems in and out of Equilibrium with the Variational Approach, *Phys. Rev. Lett.* **121**, 026805 (2018).
- [12] O. Aharony, S. S. Gubser, J. M. Maldacena, H. Ooguri, and Y. Oz, Large N field theories, string theory and gravity, *Phys. Rep.* **323**, 183 (2000).
- [13] M. Meineri, J. Penedones, and A. Rousset, Colliders and conformal interfaces, *J. High Energy Phys.* **02** (2020) 138.
- [14] T. Quella, I. Runkel, and G. M. T. Watts, Reflection and transmission for conformal defects, *J. High Energy Phys.* **04** (2007) 095.
- [15] M. Billò, V. Goncalves, E. Lauria, and M. Meineri, Defects in conformal field theory, *J. High Energy Phys.* **04** (2016) 091.
- [16] I. Affleck and A. W. W. Ludwig, Universal Noninteger “Ground State Degeneracy” in Critical Quantum Systems, *Phys. Rev. Lett.* **67**, 161 (1991).
- [17] C. Bachas, S. Chapman, D. Ge, and G. Policastro, Energy Reflection and Transmission at 2D Holographic Interfaces, *Phys. Rev. Lett.* **125**, 231602 (2020).
- [18] S. A. Baig and A. Karch, Double brane holographic model dual to 2d ICFTs, *J. High Energy Phys.* **10** (2022) 022.
- [19] A. Karch and L. Randall, Locally localized gravity, *J. High Energy Phys.* **05** (2001) 008.
- [20] A. Karch and L. Randall, Localized Gravity in String Theory, *Phys. Rev. Lett.* **87**, 061601 (2001).
- [21] O. DeWolfe, D. Z. Freedman, and H. Ooguri, Holography and defect conformal field theories, *Phys. Rev. D* **66**, 025009 (2002).
- [22] C. Bachas, J. de Boer, R. Dijkgraaf, and H. Ooguri, Permeable conformal walls and holography, *J. High Energy Phys.* **06** (2002) 027.
- [23] D. Bak, M. Gutperle, and S. Hirano, A dilatonic deformation of AdS(5) and its field theory dual, *J. High Energy Phys.* **05** (2003) 072.
- [24] D. Z. Freedman, C. Nunez, M. Schnabl, and K. Skenderis, Fake supergravity and domain wall stability, *Phys. Rev. D* **69**, 104027 (2004).
- [25] D. Bak, M. Gutperle, and S. Hirano, Three dimensional Janus and time-dependent black holes, *J. High Energy Phys.* **02** (2007) 068.
- [26] D. Bak, M. Gutperle, and R. A. Janik, Janus black holes, *J. High Energy Phys.* **10** (2011) 056.
- [27] M. Chiodaroli, M. Gutperle, and D. Krym, Half-BPS Solutions locally asymptotic to AdS<sub>3</sub> × S<sup>3</sup> and interface conformal field theories, *J. High Energy Phys.* **02** (2010) 066.

- [28] K. Chen and M. Gutperle, Janus solutions in three-dimensional  $\mathcal{N} = 8$  gauged supergravity, *J. High Energy Phys.* **05** (2021) 008.
- [29] Y. Lozano, C. Nunez, and A. Ramirez,  $\text{AdS}_2 \times \text{S}^2 \times \text{CY}_2$  solutions in type IIB with 8 supersymmetries, *J. High Energy Phys.* **04** (2021) 110.
- [30] T. Azeyanagi, A. Karch, T. Takayanagi, and E. G. Thompson, Holographic calculation of boundary entropy, *J. High Energy Phys.* **03** (2008) 054.
- [31] T. Takayanagi, Holographic Dual of BCFT, *Phys. Rev. Lett.* **107**, 101602 (2011).
- [32] J. Estes, K. Jensen, A. O’Bannon, E. Tsatis, and T. Wrase, On holographic defect entropy, *J. High Energy Phys.* **05** (2014) 084.
- [33] E. D’Hoker and M. Gutperle, Holographic entropy and Calabi’s diastasis, *J. High Energy Phys.* **10** (2014) 093.
- [34] J. Erdmenger, M. Flory, C. Hoyos, M.-N. Newrzella, and J. M. S. Wu, Entanglement entropy in a holographic Kondo model, *Fortschr. Phys.* **64**, 109 (2016).
- [35] M. Gutperle and J. D. Miller, Entanglement entropy at holographic interfaces, *Phys. Rev. D* **93**, 026006 (2016).
- [36] M. Gutperle and A. Trivella, Note on entanglement entropy and regularization in holographic interface theories, *Phys. Rev. D* **95**, 066009 (2017).
- [37] A. Karch, Z.-X. Luo, and H.-Y. Sun, Universal relations for holographic interfaces, *J. High Energy Phys.* **09** (2021) 172.
- [38] T. Anous, M. Meineri, P. Pelliconi, and J. Sonner, Sailing past the end of the world and discovering the island, *SciPost Phys.* **13**, 075 (2022).
- [39] A. Karch and M. Wang, Universal behavior of entanglement entropies in interface CFTs from general holographic spacetimes, [arXiv:2211.09148](https://arxiv.org/abs/2211.09148).
- [40] S. Chapman, D. Ge, and G. Policastro, Holographic complexity for defects distinguishes action from volume, *J. High Energy Phys.* **05** (2019) 049.
- [41] P. Braccia, A. L. Cotrone, and E. Tonni, Complexity in the presence of a boundary, *J. High Energy Phys.* **02** (2020) 051.
- [42] Y. Sato and K. Watanabe, Does boundary distinguish complexities?, *J. High Energy Phys.* **11** (2019) 132.
- [43] J. Hernandez, R. C. Myers, and S.-M. Ruan, Quantum extremal islands made easy. Part III. Complexity on the brane, *J. High Energy Phys.* **02** (2021) 173.
- [44] R. Auzzi, S. Baiguera, S. Bonansea, G. Nardelli, and K. Toccacelo, Volume complexity for Janus  $\text{AdS}_3$  geometries, *J. High Energy Phys.* **08** (2021) 045.
- [45] S. Baiguera, S. Bonansea, and K. Toccacelo, Volume complexity for the nonsupersymmetric Janus  $\text{AdS}_5$  geometry, *Phys. Rev. D* **104**, 086030 (2021).
- [46] R. Auzzi, S. Baiguera, S. Bonansea, and G. Nardelli, Action complexity in the presence of defects and boundaries, *J. High Energy Phys.* **02** (2022) 118.
- [47] J. D. Brown and M. Henneaux, Central charges in the canonical realization of asymptotic symmetries: An example from three-dimensional gravity, *Commun. Math. Phys.* **104**, 207 (1986).
- [48] C. Bachas, Z. Chen, and V. Papadopoulos, Steady states of holographic interfaces, *J. High Energy Phys.* **11** (2021) 095.
- [49] C. Saki, J. Erlich, T. J. Hollowood, and Y. Shirman, Universal aspects of gravity localized on thick branes, *Nucl. Phys.* **B581**, 309 (2000).
- [50] C. Bachas and J. Estes, Spin-2 spectrum of defect theories, *J. High Energy Phys.* **06** (2011) 005.
- [51] A. Almheiri, N. Engelhardt, D. Marolf, and H. Maxfield, The entropy of bulk quantum fields and the entanglement wedge of an evaporating black hole, *J. High Energy Phys.* **12** (2019) 063.
- [52] G. Penington, Entanglement wedge reconstruction and the information paradox, *J. High Energy Phys.* **09** (2020) 002.
- [53] A. Almheiri, T. Hartman, J. Maldacena, E. Shaghoulian, and A. Tajdini, Replica wormholes and the entropy of Hawking radiation, *J. High Energy Phys.* **05** (2020) 013.
- [54] A. Almheiri, T. Hartman, J. Maldacena, E. Shaghoulian, and A. Tajdini, The entropy of Hawking radiation, *Rev. Mod. Phys.* **93**, 035002 (2021).
- [55] D. Bak, C. Kim, S.-H. Yi, and J. Yoon, Unitarity of entanglement and islands in two-sided Janus black holes, *J. High Energy Phys.* **01** (2021) 155.
- [56] C. F. Uhlemann, Islands and Page curves in 4d from type IIB, *J. High Energy Phys.* **08** (2021) 104.
- [57] S. Demulder, A. Gneccchi, I. Lavdas, and D. Lust, Islands and light gravitons in type IIB string theory, *J. High Energy Phys.* **02** (2023) 016.
- [58] A. Karch, H. Sun, and C. F. Uhlemann, Double holography in string theory, *J. High Energy Phys.* **10** (2022) 012.
- [59] V. Mukhanov, *Physical Foundations of Cosmology* (Cambridge University Press, Oxford, 2005).
- [60] H. J. Boonstra, K. Skenderis, and P. K. Townsend, The domain wall/QFT correspondence, *J. High Energy Phys.* **01** (1999) 003.
- [61] L. Girardello, M. Petrini, M. Porrati, and A. Zaffaroni, Novel local CFT and exact results on perturbations of  $N = 4$  super Yang Mills from  $\text{AdS}$  dynamics, *J. High Energy Phys.* **12** (1998) 022.
- [62] D. Z. Freedman, S. S. Gubser, K. Pilch, and N. P. Warner, Renormalization group flows from holography supersymmetry and a c theorem, *Adv. Theor. Math. Phys.* **3**, 363 (1999).
- [63] W. Israel, Singular hypersurfaces and thin shells in general relativity, *Il Nuovo Cimento B* (1965–1970) **44**, 1 (1966).
- [64] C. Bachas and V. Papadopoulos, Phases of holographic interfaces, *J. High Energy Phys.* **04** (2021) 262.
- [65] T. Shiromizu, K.-i. Maeda, and M. Sasaki, The Einstein equation on the 3-brane world, *Phys. Rev. D* **62**, 024012 (2000).
- [66] D. Bernard, B. Doyon, and J. Viti, Non-equilibrium conformal field theories with impurities, *J. Phys. A* **48**, 05FT01 (2015).
- [67] D. Bernard and B. Doyon, Conformal field theory out of equilibrium: A review, *J. Stat. Mech.* **06** (2016) 064005.
- [68] C. Bachas and I. Brunner, Fusion of conformal interfaces, *J. High Energy Phys.* **02** (2008) 085.
- [69] Top-down  $\text{AdS}_2$  vacua do have infinite towers of spin-2 excitations, but these come from the Kaluza-Klein reduction of the extra seven dimensions, see, e.g., [70].
- [70] K. C. Rigatos, Spin-2 operators in  $\text{AdS}_2/\text{CFT}_1$ , *J. High Energy Phys.* **06** (2023) 026.
- [71] I. Papadimitriou and K. Skenderis, Correlation functions in holographic RG flows, *J. High Energy Phys.* **10** (2004) 075.
- [72] M. Chiodaroli, M. Gutperle, and L.-Y. Hung, Boundary entropy of supersymmetric Janus solutions, *J. High Energy Phys.* **09** (2010) 082.